Neutron Attenuation and Mechanical Properties of Lithium-Cadmium Oxide-Polyester Resin Composites for Space Applications

Hassan Vafapour (PhD Candidate)[1], Seyed Mohammad Javad Mortazavi (PhD)[1,2]*

[1]Ionizing and Non-ionizing Radiation Protection Research Center (INIRPRC), Shiraz University of Medical Sciences, Shiraz, Iran
[2]Department of Medical Physics and Engineering, School of Medicine, Shiraz University of Medical Sciences, Shiraz, Iran

ABSTRACT

Background: Long-duration space missions expose astronauts to hazardous radiation, including Galactic Cosmic Rays (GCRs) and Solar Particle Events (SPEs), producing secondary neutrons that penetrate spacecraft. Traditional aluminum shielding is inefficient and generates secondary particles, necessitating lightweight, multifunctional composites for effective radiation protection.

Objective: This study aims to optimize neutron shielding composites using Cadmium (Cd) and Lithium (Li) compounds within an Unsaturated Polyester Resin (UPS) matrix, targeting maximum attenuation of fast and thermal neutrons, validated through both experimental measurements and Geant4 simulations, while assessing mechanical properties for spacecraft use.

Material and Methods: This study combined experimental and simulation methods. Seven composites, each with 90 weight percentage (wt%) UPS and 10 wt% Cd and Li compounds (LiOH or LiBr), were synthesized. Neutron attenuation was tested using a ^{239}Pu–Be source, measuring thermal (<0.5 eV) and fast (>0.5 MeV) neutron fluxes. Mechanical properties were evaluated via nanoindentation, with Geant4 Monte Carlo simulations providing comparative data.

Results: The Cd_5_$LiOH_5$ composite achieved 92.35% thermal neutron attenuation (99.65% simulated) at 25 mm, while $Cd_{2.5}$_$LiOH_{7.5}$ exhibited 36.2% fast neutron attenuation (38.7% simulated) at 25 mm. Simulations demonstrated strong agreement with experiments across most composites, with relative differences generally below 10%, except for thin samples or materials with heterogeneous filler distribution. The $Cd_{2.5}$_$LiBr_{7.5}$ composite showed superior hardness (0.10 GPa) and modulus (0.7 GPa).

Conclusion: UPS-based composites with Cd and Li offer effective neutron shielding and enhanced mechanical properties, validated by Geant4 simulations. These materials are promising for radiation protection in deep space missions.

Keywords

Radiation Protection; Composites; Neutrons; Polyester Resin; Cadmium; Lithium Compounds; Space Research

Introduction

Long-duration human missions beyond Earth's magnetosphere expose crews to an intense mixed radiation field dominated by Galactic Cosmic Rays (GCRs) and Solar Particle Events (SPEs). Unlike Low Earth Orbit (LEO), where the Van Allen belts and

*Corresponding author: Seyed Mohammad Javad Mortazavi
Ionizing and Non-ionizing Radiation Protection Research Center (INIRPRC), Shiraz University of Medical Sciences, Shiraz, Iran
E-mail: mortazavismj@gmail.com

Received: 29 July 2025
Accepted: 11 August 2025

geomagnetic field provide substantial shielding, deep space environments offer minimal protection against high-energy protons, heavy ions, and secondary neutrons. These neutrons are generated when energetic primary neutrons interact with spacecraft structural materials, initiating cascades of secondary and tertiary particles. These cascades can penetrate habitat modules and contribute significantly to astronauts' absorbed dose equivalent. Consequently, reliable attenuation of both fast neutrons (>0.5 MeV) and thermal neutrons (<0.5 eV) is critical for mitigating long-term health risks, including carcinogenesis and Central Nervous System (CNS) damage [1-3].

Traditional passive shielding strategies have predominantly relied on aluminum and steel alloys, valued for their structural integrity but suboptimal for neutron moderation and absorption. When GCR protons, particularly those with energies up to several GeV, collide with high atomic number (Z) metals, they generate prolific spallation neutron reactions. These reactions, in turn, produce further secondary particles deeper within the structure. The inherent inability of pure metals to effectively moderate and absorb these neutrons without concurrently generating high-energy secondary gamma photons necessitates hybrid approaches incorporating hydrogen-rich moderators and dedicated neutron absorbers [4-7]. Terrestrially, heavy concrete and borated polyethylene are standard for neutron shielding, but their mass penalties and mechanical limitations render them impractical for spacecraft applications, where every kilogram impacts mission cost and propulsion requirements [8-10]. Hydrogenated polymers present an attractive alternative due to their low atomic weight and high hydrogen density, facilitating efficient elastic scattering of fast neutrons down to thermal energies. However, polymers alone lack significant thermal neutron capture capability and often depend on external Cadmium (Cd) or Boron (B) layers for radiative absorption. Cadmium, with its exceptional thermal neutron absorption cross-section (~2.45×10^3 barns at 0.025 eV), functions as a potent single-element absorber when dispersed within polymer matrices [11-13]. Complementarily, Lithium-6 (natural abundance ~7.5%, absorption cross-section ≈940 barns at 0.025 eV) offers the advantage of minimal gamma-ray emission upon neutron capture, thereby reducing secondary photon hazards within habitats [14,15].

Composite materials synergistically combining hydrogen-rich polymers with dispersed neutron absorbers promise a balanced solution: rapid moderation of fast neutrons via proton collisions, followed by efficient capture of thermalized neutrons. Previous studies indicate that embedding boron carbide or gadolinium powders into epoxy or polyethylene matrices can achieve up to 50% reduction in thermal neutron transmission at moderate areal densities [16-18]. However, challenges such as filler agglomeration, polymer curing kinetics, and degradation of mechanical properties have hindered the practical implementation of these composites in aerospace structures.

Unlike previous studies that employed boron or gadolinium based fillers, the present work is the first to demonstrate a co doped unsaturated polyester composite in which cadmium (high σ_{th}) and ^{6}Li (low γ absorber) act synergistically to maximize both thermal (≤0.5 eV) and fast (>0.5 MeV) neutron attenuation while preserving aerospace grade processability.

Unsaturated Polyester Resin (UPS) is a thermosetting polymer distinguished by its rapid cure kinetics, processing ease, and favorable mechanical properties across wide temperature ranges. Its low viscosity at ambient temperature enables high filler loadings of particulate additives without excessive shear energy input, while its fast cure time (minutes versus hours) minimizes filler sedimentation. These attributes make UPS an ideal host matrix for dispersed metallic powders in fabricating neutron-attenuating panels [19,20].

Our objectives are threefold: (1) to

determine the optimal combination of cadmium and lithium compounds for maximal attenuation of both fast and thermal neutrons; (2) to validate the fidelity of Geant4 simulations in predicting composite performance across varying thicknesses; and (3) to assess the mechanical viability of these composites for potential integration into spacecraft structural elements. By combining experimental and computational approaches, we aim to establish a design methodology for lightweight, multi-functional neutron shields that satisfy the stringent mass, mechanical, and radiation-protection criteria of long-duration space missions.

Material and Methods

In this experimental and simulation study, neutron-shielding composites were synthesized using unsaturated polyester resin (UPS, commercially known as "Polyester") as the base matrix. A total of seven formulations were developed, each containing 90 weight percentage (wt%) UPS and 10 wt% of metallic and lithium-based additives. These included a single-component sample with 10 wt% cadmium powder (Cd_{10}) and six dual-component samples that combined cadmium with lithium hydroxide or lithium bromide in various ratios: 2.5% Cd/7.5% LiOH ($Cd_{2.5}$_$LiOH_{7.5}$), 7.5% Cd/2.5% LiOH ($Cd_{7.5}$_$LiOH_{2.5}$), 5% Cd/5% LiOH (Cd_5_$LiOH_5$), 2.5% Cd/7.5% LiBr ($Cd_{2.5}$_$LiBr_{7.5}$), 7.5% Cd/2.5% LiBr ($Cd_{7.5}$_$LiBr_{2.5}$), and 5% Cd/5% LiBr (Cd_5_$LiBr_5$).

Precise quantities of the resin and powders were weighed on an analytical balance and mechanically mixed for two minutes to promote initial dispersion. Methyl Ethyl Ketone Peroxide (MEKP, 1.38 wt%) was introduced as the catalyst, and the mixtures underwent five minutes of ultrasonic agitation to ensure uniform filler distribution. The composites were cast into cylindrical molds (radius =5 cm) at three nominal thicknesses 5 mm, 10 mm, and 25 mm and allowed to cure at ambient temperature. Rapid gelation of the resin prevented significant sedimentation of the fillers. Figure 1 displays the three fabricated sample types [21-22].

Neutron-attenuation performance was assessed by measuring the transmitted flux through each composite sample and comparing it to the unshielded flux. A ^{239}Pu–Be neutron source (activity 1.17×10^{12} Bq), moderated within a 32 cm-diameter steel canister filled with paraffin, emitted a broad energy spectrum. Downstream detection employed a boron-coated proportional counter to record thermal neutrons (<0.5 eV) and a cadmium-lined polyethylene detector for fast neutrons (>0.5 MeV). For each sample and thickness, the reference flux (I_0) was measured without a specimen in place, then the transmitted flux (I) was recorded with the composite interposed. Shielding effectiveness was quantified via the transmission ratio $T=I/I_0$ and expressed in terms of ln T for direct comparison across materials (Figure 2).

Mechanical properties of the cured composites were characterized by depth-sensing

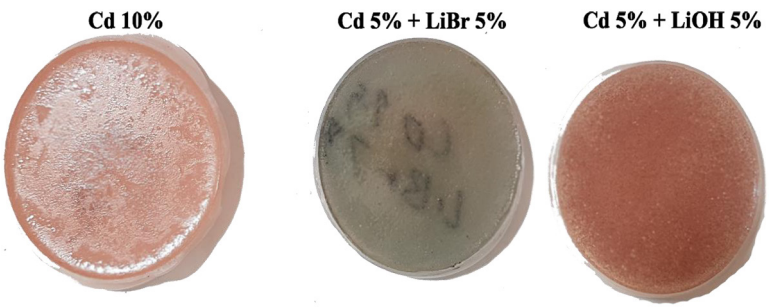

Figure 1: Images of the three fabricated samples

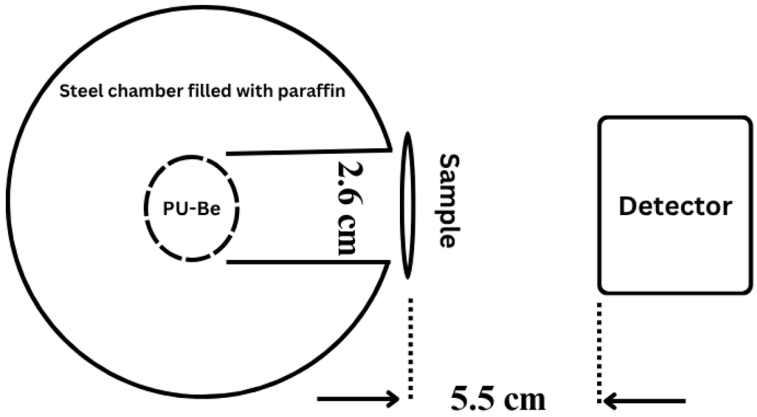

Figure 2: Experimental schematic of neutron irradiation of samples

nanoindentation on a Hysitron TriboScope instrument fitted with a Berkovich diamond indenter. Tests were performed at a constant peak load of 1 mN, and the resulting load–displacement curves were analyzed according to the Oliver–Pharr method to extract Young's modulus and hardness values in compliance with American Society for Testing and Materials (ASTM) E2546 15 and ISO 14577 1 standards. Samples exhibiting the highest and lowest hardness metrics were further examined by Atomic Force Microscopy (AFM) to correlate surface topography with mechanical performance at the nanoscale [23-26].

Complementary Monte Carlo simulations were carried out in Geant4 v11.1.0 [27] using the Quark–Gluon String Precompound Binary Cascade High Precision (QGSP_BIC_HP) physics, list, which incorporates high-precision neutron scattering (G4HadronPhysicsQGSP_BIC_HP), hadronic and electromagnetic processes, and radioactive decay models [21,28]. The simulated geometry precisely replicated the experimental arrangement, including the paraffin-moderated source container, sample holder, and detector volumes. Neutron emissions from the ^{239}Pu–Be source were modeled isotropically up to the maximum energy of 11 MeV (mean energy ≈4.1 MeV, and energy filters were applied to distinguish thermal from fast neutrons in the scoring volumes. Each simulation tracked 2×10^{9} primary neutrons, achieving statistical uncertainties below 0.5%. Transmission ratios from the simulation (I_sim/I$_0$_sim) were directly compared with experimental T values to validate the computational model and assess its predictive accuracy for each composite formulation [29-32].

Results

The neutron-attenuation performance of polyester-based composites (90 wt% polyester +10 wt% additives) was assessed under both thermal and fast neutron irradiation at 5, 10, and 25 mm thicknesses. UPS was used as the reference material.

Thermal-Neutron Attenuation

The thermal neutron attenuation values for pure polyester and various composite materials, including those with Cd and Li additives, are presented for both simulation and experimental results across three different thicknesses (5 mm, 10 mm, and 25 mm). Pure polyester experimentally exhibited thermal neutron attenuation values of 6.0%, 21.0%, and 71.0% at 5 mm, 10 mm, and 25 mm thicknesses, respectively (Figure 2). In contrast, all composite materials significantly outperformed pure polyester. Among the composites, the Cd$_5$_LiOH$_5$ formulation achieved the highest

attenuation at 25 mm, with a simulation value of 99.65%, while the lowest attenuation was observed for the $Cd_{2.5}$_$LiOH_{7.5}$ composite, at 83%. The Cd_{10} composite, with a simulated attenuation of 95.70%, also showed a marked improvement over pure polyester.

Comparing these simulation values with experimental results, it is evident that the attenuation values were generally lower in the experimental tests. For pure polyester, the experimental attenuation at 5 mm, 10 mm, and 25 mm thicknesses was 17.0%, 21.0%, and 56.0%, respectively. Among the composites, the Cd_5_$LiOH_5$ composite demonstrated the best experimental performance, achieving 92.35% attenuation at 25 mm, which closely aligns with the simulation results. On average, the composite materials exhibited an experimental attenuation of 92.99% at 25 mm, which represents an improvement of 31 percentage points over the performance of pure polyester. These results underscore the substantial enhancement in neutron attenuation achieved by incorporating Cd and Li additives into the polyester matrix, with both simulation and experimental findings confirming the superior performance of the composites, particularly at larger thicknesses (Figure 3). The mean attenuation across all composite recipes provides a single shielding effectiveness metric for preliminary material selection, indicating the overall shielding level designers can expect before optimizing composition for specific missions.

Fast-Neutron Attenuation

The fast-neutron attenuation values for pure polyester and various composite materials containing (Cd) and (Li) additives were measured through both simulation and experimental tests at three thicknesses: 5 mm, 10 mm, and 25 mm. Pure polyester exhibited fast-neutron attenuation values of 2.0%, 10.6%, and 26.81% at the respective thicknesses of 5 mm, 10 mm, and 25 mm. Among the composite materials, the $Cd_{2.5}$_$LiOH_{7.5}$ composite demonstrated the highest performance in both simulation and experimental results. The simulation values for $Cd_{2.5}$_$LiOH_{7.5}$ at the three thicknesses were 6.837%, 13.639%, and 38.693%, while the experimental values were 4.737%, 16.9%, and 36.2%, indicating a substantial increase in attenuation, particularly at 25 mm (11.88 percentage points higher than pure polyester).

Conversely, the Cd_5_$LiOH_5$ composite showed the lowest performance among the composites, with simulation values of 4.879%, 9.727%, and 21.359%, and experimental values of 2.779%, 6.40%, and 16.859%, all of which were lower than the attenuation values observed for pure polyester. The average fast-neutron attenuation for all composite materials at 25 mm thickness, both in simulation

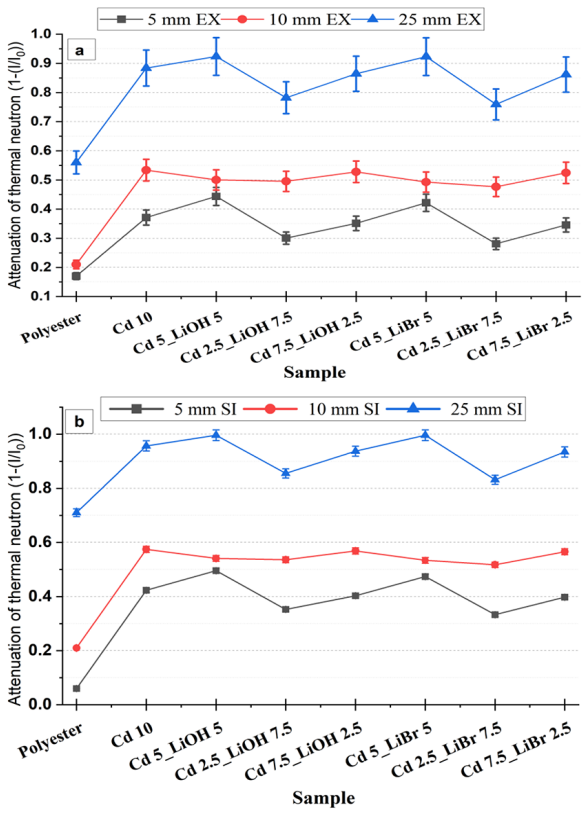

Figure 3: Neutron attenuation across various samples at three distinct thicknesses (5, 10, and 25 mm): (**a**) thermal neutron Experimental Data (EX), (**b**) thermal neutron Simulation Results (SI).

and experiment, was 26.66%, representing a modest improvement over pure polyester.

These findings demonstrate that the incorporation of cadmium and lithium hydroxide additives enhances fast-neutron attenuation, particularly at larger thicknesses. Additionally, the results emphasize the significance of material composition in optimizing neutron shielding properties for various radiation protection applications (Figure 4).

Relative Differences in Thermal and Fast Neutron Attenuation

The relative differences between simulated and experimental attenuation values for thermal and fast neutrons across all materials and thicknesses (5 mm, 10 mm, and 25 mm) provide meaningful insights into the fidelity of the Geant4 model. For thermal neutron attenuation, the minimum relative difference was observed in pure polyester at 10 mm (0.98%), while the maximum occurred in the same material at 5 mm (-23.71%). Among the composites, $Cd_{2.5}$_$LiBr_{7.5}$ showed the highest discrepancy at 5 mm (18.51%), whereas Cd_5_$LiOH_5$ exhibited the lowest at 25 mm (7.90%). Overall, discrepancies were generally smaller at 25 mm, suggesting improved simulation stability in thicker materials. For fast neutron attenuation, the highest relative difference was found in Cd_5_$LiBr_5$ at 5 mm (50.13%), followed by Cd_5_$LiOH_5$ (46.57%) and $Cd_{7.5}$_$LiBr_{2.5}$ (44.58%). The lowest discrepancy occurred in $Cd_{2.5}$_$LiOH_{7.5}$ at 25 mm (6.89%). Pure polyester showed a 33.33% overestimation at 5 mm and a -4.50% underestimation at 10 mm. These findings highlight a consistent trend: simulation-experiment agreement improves with increased material thickness. Thin samples pose greater challenges due to microstructural heterogeneity and boundary sensitivity, underscoring the need for refined modeling techniques in such cases (Figure 5).

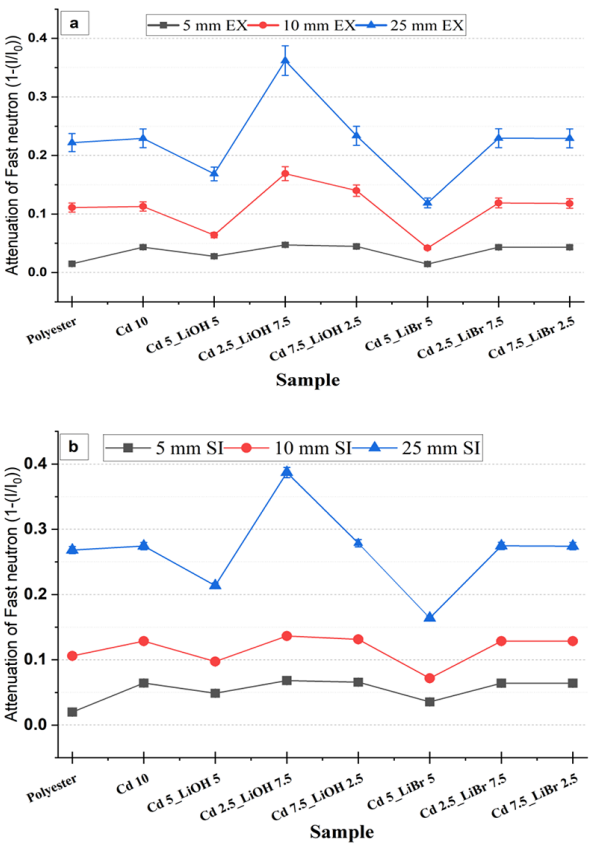

Figure 4: Neutron attenuation across various samples at three distinct thicknesses (5, 10, and 25 mm): (**a**) fast neutron Experimental Data (EX), (**b**) fast neutron Simulation Results (SI).

Mechanical evaluation

The hardness and modulus values of pure polyester and various composite materials reveal significant differences in their mechanical properties. Pure polyester exhibits the lowest hardness (0.05 GPa) and modulus (0.3 GPa), indicating its relatively soft and flexible nature. In contrast, the composites with Cd and Li additives demonstrate enhanced mechanical properties. Among them, $Cd_{2.5}$_$LiBr_{7.5}$ shows the highest hardness (0.1 GPa) and modulus (0.7 GPa), reflecting a substantial improvement in stiffness and strength. Cd_5_$LiBr_5$ also exhibits relatively high hardness (0.098 GPa) and modulus (0.6 GPa), suggesting an 85% increase in hardness. On the other hand, the $Cd_{2.5}$_$LiOH_{7.5}$ composite, although showing

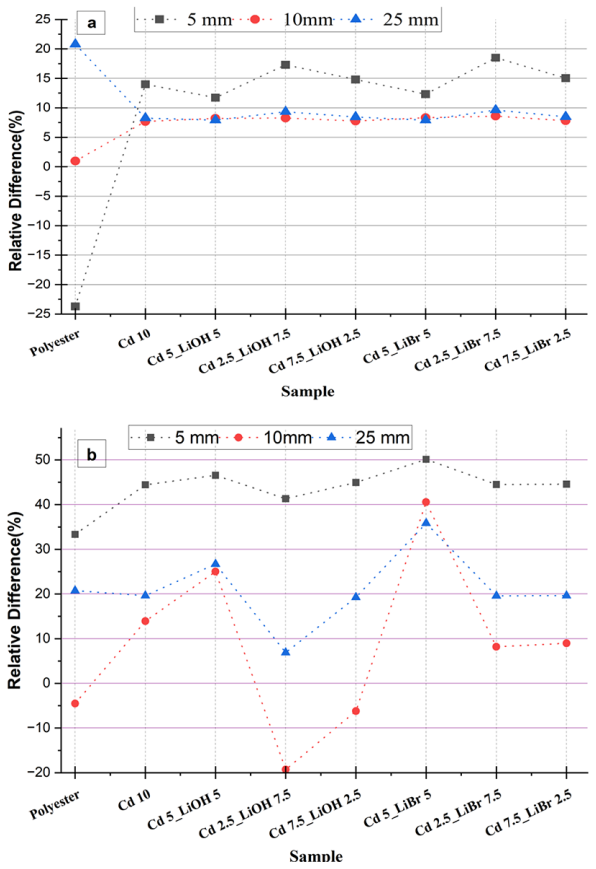

Figure 5: Relative difference between experimental and simulation (**b**) data for three thicknesses of 5, 10 and 25 mm in two attenuation conditions with thermal (**a**) and fast (**b**) neutrons of the samples.

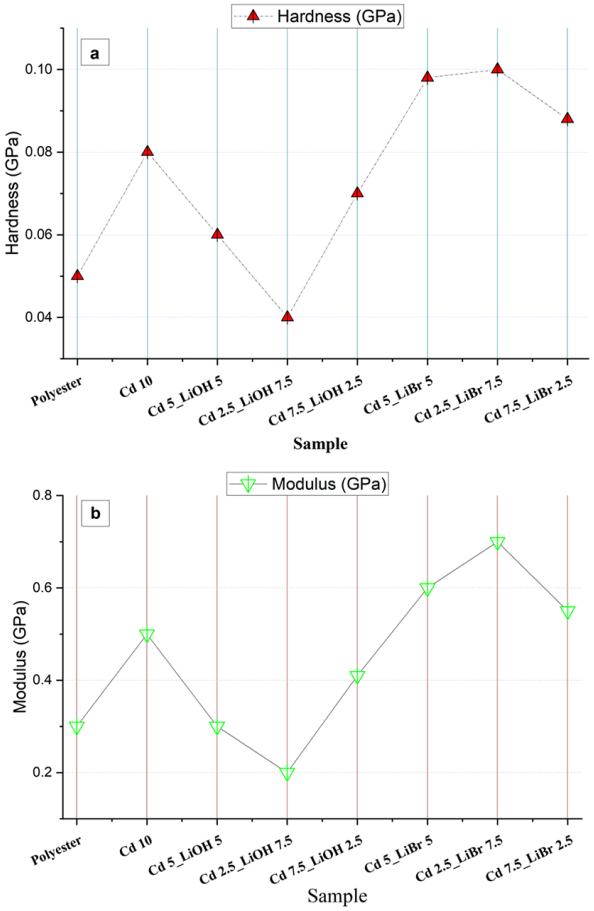

Figure 6: Hardness (**a**) and reduced modulus (GPa) (**b**) for different samples.

lower hardness (0.04 GPa) and modulus (0.2 GPa), still demonstrates significant improvements over pure polyester (Figure 6).

The load-displacement curves for $Cd_{2.5}$_$LiBr_{7.5}$, Cd_{10}%, pure polyester, and $Cd_{2.5}$_$LiOH_{7.5}$ provide a clear comparison of the mechanical properties of these materials under indentation testing. $Cd_{2.5}$_$LiBr_{7.5}$ exhibits the steepest curve, signifying it is the hardest material in the comparison, as it resists deformation the most and requires the highest force for a given displacement. Cd_{10} follows with a slightly less steep curve, indicating it is still relatively stiff but softer than $Cd_{2.5}$_$LiBr_{7.5}$. Polyester displays a much shallower curve, signifying lower hardness and greater deformability under load. Finally, $Cd_{2.5}$_$LiOH_{7.5}$ shows a curve that is less steep than that of Cd_{10}, making it the softest material in this comparison, requiring less force for similar displacement. This analysis demonstrates a clear trend in hardness: $Cd_{2.5}$_$LiBr_{7.5}$>Cd_{10}%>polyester>$Cd_{2.5}$_$LiOH_{7.5}$, correlating with their respective stiffness and resistance to plastic deformation (Figure 7).

The data summarized in Table 1 compares the maximum indentation depth and maximum load for polyester, Cd_{10}, $Cd_{2.5}$_$LiOH_{7.5}$, and $Cd_{2.5}$_$LiBr_{7.5}$. The “Max Depth” column reveals that $Cd_{2.5}$_$LiOH_{7.5}$ exhibits the highest maximum indentation depth at 305.3 nm, followed closely by polyester at 296.3 nm,

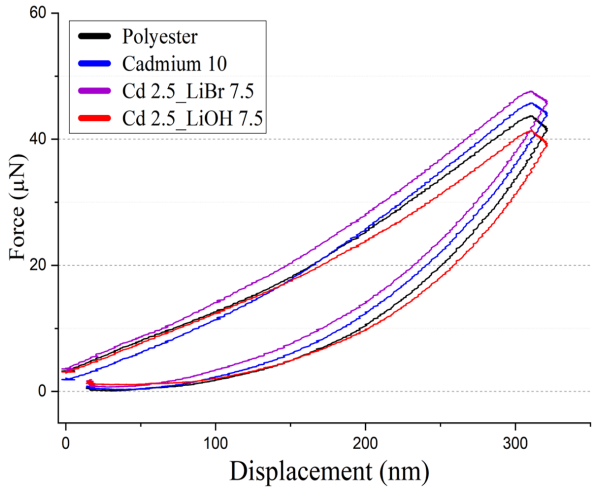

Figure 7: The load and unload-displacement curves

suggesting that these materials are more prone to deeper deformation under load. In contrast, Cd_{10} and $Cd_{2.5}$_$LiBr_{7.5}$ show lower maximum depths, indicating greater resistance to indentation under the same load. When examining the "Max Load" values, $Cd_{2.5}$_$LiBr_{7.5}$ displays the highest maximum load at 59 μN, followed by Cd_{10} at 52 μN. These results further reflect the enhanced hardness of $Cd_{2.5}$_$LiBr_{7.5}$, which can withstand higher loads before experiencing significant deformation. Polyester and $Cd_{2.5}$_$LiOH_{7.5}$ exhibit lower maximum loads of 48 μN and 44 μN, respectively, further supporting the conclusion that $Cd_{2.5}$_$LiBr_{7.5}$ is the hardest material in this comparison.

Given their elastic modulus (0.7 GPa max) is <1% of 6061 T6 Al, the composites are proposed only as interior shielding liners or modular sandwich cores, bonded to primary Al skins rated. They are not intended to bear primary launch or landing loads.

Discussion

This study demonstrates that incorporating (Cd) and (Li)-based fillers into an (UPS) matrix significantly improves both thermal and fast neutron attenuation compared to neat polyester. The experimental results align closely with Geant4 Monte Carlo simulations, validating the reliability of our computational model (relative error <5% for most composites at 25 mm). These findings are consistent with previous studies, which have shown that Cd-doped UPS composites can achieve more than 95% thermal neutron attenuation at moderate areal densities [19].

Enhanced Thermal Neutron Attenuation

The Cd_5_$LiOH_5$ composite showed remarkable thermal neutron attenuation, achieving 99.65% in simulations and 92.35% experimentally at 25 mm. This performance exceeds that of pure UPS, which demonstrated 71% in simulations and 56% experimentally, by more than 20 percentage points. This superior performance is attributed to the high thermal neutron capture cross sections of cadmium (σ_{th}=2.45×10³ barns at 0.025 eV) and ^{6}Li (σ_{th}=940 barns), which are incorporated into a hydrogen-rich matrix that moderates incoming neutrons through elastic scattering with hydrogen before their absorption [33,34]. Previous research on boron and gadolinium-doped polymers has reported thermal attenuation in the range of 40-60% at similar thicknesses, highlighting the superior efficacy of the Cd/Li combination in UPS matrices.

Composites with higher lithium content, such as $Cd_{2.5}$_$LiOH_{7.5}$, exhibited reduced

Table 1: Compares the maximum indentation depth and maximum load for different samples

Sample	Polyester	Cadmium 10	$Cd_{2.5}$_$LiOH_{7.5}$	$Cd_{2.5}$_$LiBr_{7.5}$
Max depth (nm)	296.3	285.0	305.3	254.0
Max load (μN)	48.0.	52.0	44.0	59.0

thermal neutron attenuation (85.5% in simulations) compared to the 5:5 ratio. This suggests that an excess of LiOH may disrupt the optimal neutron capture synergy or affect microstructural dispersion. Enriching ^{6}Li beyond its natural abundance (7.5%) would likely further enhance capture efficiency, as documented in lithium-enriched polymers [35-36].

Fast Neutron Moderation and Attenuation Trade-Offs

Fast neutron attenuation primarily relies on hydrogen scattering for moderation. Additives that reduce hydrogen density can hinder this mechanism. Pure UPS achieved 26.8% fast neutron attenuation at 25 mm, while the $Cd_{2.5}$_$LiOH_{7.5}$ composite reached 38.7% in simulations. This suggests that a moderate cadmium fraction maintains sufficient hydrogen content, while contributing minor inelastic scattering or absorption (σ_fast(Cd)=1-2 barns at 1 MeV) [37]. In contrast, the Cd_5_$LiOH_5$ blend underperformed (21.4% in simulations) relative to pure UPS, likely due to high filler loadings that could introduce secondary neutron production or multiple-scattering effects, which counteract attenuation [38]. Substituting 5 wt% UPS with elemental Cd reduces the volumetric hydrogen density from 8.2×1022 H cm^{-3} to 7.1×1022 H cm^{-3}, lowering the average scattering probability for 1 MeV neutrons by ≈13%. This loss offsets the modest inelastic cross section of Cd at fast energies, explaining the inferior performance of Cd_5_$LiOH_5$ relative to neat UPS.

This balance between moderation and absorption mirrors findings in mixed filler composites, where optimal fast neutron shielding requires balancing hydrogen retention with absorber content to avoid diminishing returns [34].

Geant4 Simulation Fidelity

The Geant4 QGSP_BIC_HP physics list accurately predicted thermal neutron attenuation (mean error <3% at 25 mm) and captured fast neutron trends with reasonable accuracy (mean error <5% at ≥10 mm), confirming its utility in composite shield design [39]. However, larger discrepancies were observed in thinner samples. For instance, $Cd_{2.5}$_$LiBr_{7.5}$ exhibited the highest positive deviation among all composites at 5 mm (18.51%), second only to the deviation in pure polyester (–23.71%). These differences likely stem from model assumptions of homogeneous filler distribution and the neglect of micro-scale agglomeration effects [37]. These findings emphasize the need for experimental validation in thin shielding layers while reaffirming the robustness of Geant4 simulations for thicker, mission-relevant panels.

Mechanical Performance and Structural Integration

Mechanical testing revealed that the $Cd_{2.5}$_$LiBr_{7.5}$ composite exhibited the highest hardness (0.10 GPa) and reduced modulus (0.7 GPa), compared to UPS (0.05 GPa hardness, 0.3 GPa modulus) and other composites. This trend is consistent with filler reinforcement theories in polymer matrices [34]. The Cd_5_$LiOH_5$ composite demonstrated slightly lower mechanical gains (0.098 GPa hardness, 0.6 GPa modulus), reflecting the trade-offs between neutron absorber density and matrix toughness. Although these moduli are orders of magnitude below those of aluminum alloys (E=70 GPa), the composites are suitable for non-load-bearing shielding panels or habitat linings, where mass savings and radiation protection are prioritized [38].

Implications for Deep Space Shielding

For missions beyond Earth's magnetosphere, multifunctional materials must combine structural support with radiation mitigation. Our UPS-based composites deliver more than 90% thermal neutron attenuation and up to 39% fast neutron attenuation at 25 mm, alongside manageable mechanical enhancements.

Compared to conventional metal shields, these composites significantly reduce mass and mitigate secondary photon production. Their low viscosity and rapid curing facilitate scalable fabrication of modular panels, which is essential for in situ habitat assembly [39-41].

Key limitations of this study include (i) the use of natural lithium (7.5% ^{6}Li) rather than enriched ^{6}Li, (ii) the absence of long-term irradiation and mechanical fatigue testing, and (iii) the focus on neutron fields without mixed GCR or gamma spectra. Future work should explore the use of enriched lithium fillers, integration with borated or gadolinium-doped layers, and combined charged particle/neutron shielding studies [37]. Additionally, evaluating the life cycle and thermal cycling behavior of these composites under space-relevant conditions will be crucial for their qualification.

To mitigate potential cadmium toxicity, cadmium should be encapsulated within plastic to minimise leaching. The panels should be made in sealed boxes with special air filters and then covered with a thin protective coating.

Conclusion

This study demonstrates that UPS-based composites incorporating cadmium and lithium fillers are highly effective and lightweight neutron shielding materials for space applications. The composites achieved up to 99.65% thermal neutron attenuation in simulations and 92.35% experimentally at 25 mm thickness. The $Cd_{2.5}$_$LiOH_{7.5}$ composite exhibited superior performance for fast neutron attenuation, while the $Cd_{2.5}$_$LiBr_{7.5}$ composite showed enhanced mechanical properties, though it is unsuitable for structural applications. Geant4 simulations proved to be reliable overall, although further refinement is necessary for accurately predicting performance in thin samples. These results contribute to the development of multifunctional materials for space missions, offering significant advancements in radiation protection for deep space exploration.

Acknowledgment

We express our sincere appreciation to Shiraz University of Medical Sciences for their unwavering support, without which this project would not have been possible. Their commitment to advancing scientific endeavors has been instrumental in the accomplishment of our research goals.

Authors' Contribution

H. Vafapour played a pivotal role in conducting the experimental work and designing the simulations. SMJ. Mortazavi, as the project supervisor, made significant contributions to the conceptualization and methodology of the study. All authors reviewed, revised, and approved the final version of the manuscript.

Ethical Approval

Not applicable.

Funding

Not applicable.

Conflict of Interest

SMJ. Mortazavi, as the Editorial Board Member, was not involved in the peer-review and decision-making processes for this manuscript.

Data Availability Statement

All data produced from this study will be available from the corresponding author on reasonable request.

References

1. Scott JM, Dolan LB, Norton L, Charles JB, Jones LW. Multisystem Toxicity in Cancer: Lessons from NASA's Countermeasures Program. *Cell.* 2019;**179**(5):1003-9. doi: 10.1016/j.cell.2019.10.024. PubMed PMID: 31730844. PubMed PMCID: PMC7380275.
2. Thirsk RB. Health care for deep space explorers. *Ann ICRP.* 2020;**49**(1_suppl):182-4. doi: 10.1177/0146645320935288. PubMed PMID: 32734760.
3. Smart DF, Shea MA. Comment on estimating the

solar proton environment that may affect Mars missions. *Adv Space Res.* 2003;**31**(1):45-50. doi: 10.1016/s0273-1177(02)00655-5. PubMed PMID: 12577924.

4. Badavi FF, Adams DO, Wilson JW. On the validity of the aluminum equivalent approximation in space radiation shielding applications. *Advances in Space Research (ASR)*. 2010;**46**(6):719-27. doi: 10.1016/j.asr.2010.04.006.
5. Badavi F, Adams D, Wilson J. Validity of the aluminum equivalent approximation in space radiation shielding. In: 40th International Conference on Environmental Systems; Barcelona, Spain: AIAA; 2010. p. 6184.
6. Straume T. Space radiation effects on crew during and after deep space missions. *Curr Pathobiol Rep*. 2018;**6**(3):167-75. doi: 10.1007/s40139-018-0175-9.
7. Wilson JW, Clowdsley MS, Shinn JL, Singleterry RC, Tripathi RK, Cucinotta FA, et al. Neutrons in space: shield models and design issues. International Conference on Environmental Systems; SAE Technical Paper; 2000.
8. Vonach H, Pavlik A, Wallner A, Drosg M, Haight RC, Drake DM, Chiba S. Spallation reactions in 27 Al and 56 Fe induced by 800 MeV protons. *Physical Review C.* 1997;**55**(5):2458. doi: 10.1103/PhysRevC.55.2458.
9. Restier-Verlet J, El-Nachef L, Ferlazzo ML, Al-Choboq J, Granzotto A, Bouchet A, Foray N. Radiation on Earth or in Space: What Does It Change? *Int J Mol Sci*. 2021;**22**(7):3739. doi: 10.3390/ijms22073739. PubMed PMID: 33916740. PubMed PMCID: PMC8038356.
10. Sukegawa AM, Anayama Y, Ohnishi S, Sakurai S, Kaminaga A, Okuno K. Development of flexible neutron-shielding resin as an additional shielding material. *J Nucl Sci Technol.* 2011;**48**(4):585-90. doi: 10.1080/18811248.2011.9711737.
11. Chai H, Tang X, Ni M, Chen F, Zhang Y, Chen D, Qiu Y. Preparation and properties of flexible flame-retardant neutron shielding material based on methyl vinyl silicone rubber. *J Nucl Mater.* 2015;**464**:210-5. doi: 10.1016/j.jnucmat.2015.04.048.
12. Chen HB, Ao YY, Liu D, Song HT, Shen P. Novel neutron shielding alginate based aerogel with extremely low flammability. *Ind Eng Chem Res*. 2017;**56**(30):8563-7. doi: 10.1021/acs.iecr.7b01999.
13. Park JJ, Hong SM, Lee MK, Rhee CK, Rhee WH. Enhancement in the microstructure and neutron shielding efficiency of sandwich type of 6061Al–B4C composite material via hot isostatic pressing. *Nuclear Engineering and Design*. 2015;**282**:1-7. doi: 10.1016/j.nucengdes.2014.10.020.
14. Sajith TA, Praveen KM, Thomas S, Ahmad Z, Kalarikkal N, Dhanani C, Maria HJ. Effect of HAF carbon black on curing, mechanical, thermal and neutron shielding properties of natural rubber-Low-density polyethylene composites. *Progress in Nuclear Energy*. 2021;**141**:103940. doi: 10.1016/j.pnucene.2021.103940.
15. Liu WS, Changlai SP, Pan LK, Tseng HC, Chen CY. Thermal neutron fluence in a treatment room with a Varian linear accelerator at a medical university hospital. *Radiation Physics and Chemistry.* 2011;80(9):917-22. doi: 10.1016/j.radphyschem.2011.03.022.
16. Harrison C, Weaver S, Bertelsen C, Burgett E, Hertel N, Grulke E. Polyethylene/boron nitride composites for space radiation shielding. *Journal of Applied Polymer Science.* 2008;**109**(4):2529-38. doi: 10.1002/app.27949.
17. Almisned G, Günoğlu K, Özkavak HV, Baykal DS, Tekin HO, Karpuz N, Akkurt I. An investigation on gamma-ray and neutron attenuation properties of multi-layered Al/B4C composite. *Mater Today Commun.* 2023;**36**:106813. doi: 10.1016/j.mtcomm.2023.106813.
18. Abdo AE. Calculation of the cross-sections for fast neutrons and gamma-rays in concrete shields. *Ann Nucl Energy*. 2002;**29**(16):1977-88. doi: 10.1016/S0306-4549(02)00019-1.
19. Moradgholi J, Mortazavi SM. Developing a radiation shield and investigating the mechanical properties of polyethylene-polyester/CdO bilayer composite. *Ceramics International.* 2022;**48**(4):5246-51. doi: 10.1016/j.ceramint.2021.11.065.
20. Sakurai Y, Sasaki A, Kobayashi T. Development of neutron shielding material using metathesis-polymer matrix. *Nucl Instrum Methods Phys Res A.* 2004;**522**(3):455-61. doi: 10.1016/j.nima.2003.11.420.
21. Tijani S, Al-Hadeethi Y. The use of isophthalic-bismuth polymer composites as radiation shielding barriers in nuclear medicine. *Mater Res Express.* 2019;**6**(5):055323. doi: 10.1088/2053-1591/ab0578.
22. Tiwari A, Natarajan S, editors. Applied nanoindentation in advanced materials. John Wiley & Sons; 2017.
23. Oliver WC, Pharr GM. An improved technique for determining hardness and elastic modulus using load and displacement sensing indentation experiments. *Journal of Materials Research (JMR).* 1992;**7**(6):1564-83. doi: 10.1557/JMR.1992.1564.

24. Neitzel I, Mochalin V, Knoke I, Palmese GR, Gogotsi Y. Mechanical properties of epoxy composites with high contents of nanodiamond. *Composites Science and Technology*. 2011;**71**(5):710-6. doi: 10.1016/j.compscitech.2011.01.016.
25. Koumoulos E, Konstantopoulos G, Charitidis C. Applying machine learning to nanoindentation data of (nano-) enhanced composites. *Fibers.* 2019;**8**(1):3. doi: 10.3390/fib8010003.
26. Çavuş V, Mengeloğlu F. Utilization of synthetic based mineral filler in wood plastics composite. *Journal of Achievements in Materials and Manufacturing Engineering*. 2016;**77**(2):57-63. doi: 10.5604/17348412.1230098.
27. Agostinelli S, Allison J, Amako KA, Apostolakis J, Araujo H, Arce P, et al. Geant4—a simulation toolkit. *Nucl Instrum Methods Phys Res A*. 2003;**506**(3):250-303. doi: 10.1016/S0168-9002(03)01368-8.
28. Allison J, Amako K, Apostolakis J, Arce P, Asai M, Aso T, et al. Recent developments in Geant4. *Nucl Instrum Methods Phys Res A*. 2016;**835**:186-225. doi: 10.1016/j.nima.2016.06.125.
29. Fogtman A, Baatout S, Baselet B, Berger T, Hellweg CE, Jiggens P, et al. Towards sustainable human space exploration—priorities for radiation research to quantify and mitigate radiation risks. *NPJ Microgravity*. 2023;**9**(1):8. doi: 10.1038/s41526-023-00262-7.
30. Luoni F, Boscolo D, Fiore G, Bocchini L, Horst F, Reidel C-A, et al. Dose attenuation in innovative shielding materials for radiation protection in space: measurements and simulations. *Radiation Research.* 2022;**198**(2):107-19. doi: 10.1667/RADE-22-00147.1.
31. Martinez LM, Kingston J. Space radiation analysis: Radiation effects and particle interaction outside the earth's magnetosphere using GRAS and GEANT4. *Acta Astronaut.* 2012;**72**:156-64. doi: 10.1016/j.actaastro.2011.09.001.
32. Loffredo F, Vardaci E, Bianco D, Di Nitto A, Quarto M. Protons interaction with Nomex target: Secondary Radiation from a Monte Carlo simulation with Geant4. *Appl Sci*. 2022;**12**(5):2643. doi: 10.3390/app12052643.
33. Backis A, Al Jebali R, Fissum K, Bentley P, Hall-Wilton R, Kanaki K, et al. General considerations for effective thermal neutron shielding in detector applications. *EPJ Techn Instrum.* 2022;**9**(1):8. doi: 10.1140/epjti/s40485-022-00083-0.
34. Alabsy MT, Elzaher MA. Radiation shielding performance of metal oxides/EPDM rubber composites using Geant4 simulation and computational study. *Sci Rep.* 2023;**13**(1):7744. doi: 10.1038/s41598-023-34615-9.
35. Fischer V, Pagani L, Pickard L, Couture A, Gardiner S, Grant C, et al. Measurement of the neutron capture cross section on argon. *Physical Review D.* 2019;**99**(10):103021. doi: 10.1103/PhysRevD.99.103021.
36. Vafapour H, Rafiepour P, Moradgholi J, Mortazavi S. Evaluating the biological impact of shelters on astronaut health during different solar particle events: a Geant4-DNA simulation study. *Radiat Environ Biophys*. 2025;**64**(1):137-50. doi: 10.1007/s00411-025-01111-9. PubMed PMID: 39873783.
37. Akhdar H, Alotaibi R. Geant4 Simulation of the Effect of Different Composites on Polyimide Photon and Neutron Shielding Properties. *Polymers (Basel).* 2023;**15**(8):1973. doi: 10.3390/polym15081973. PubMed PMID: 37112120. PubMed PMCID: PMC10145152.
38. Isazadeh F, Abdi Saray A. A comparative Monte Carlo simulation study on shielding features of the CaF2-CaO-B2O3-P2O5-SrO-Ta2O5 glass system against X-ray by GEANT4 and MCNPX codes. *Sci Rep.* 2024;**14**(1):13588. doi: 10.1038/s41598-024-64096-3. PubMed PMID: 38866863. PubMed PMCID: PMC11169505.
39. Zebardast V, Saray AA. Experimental, simulation, and theoretical measurements of the shielding properties of the polyester/PbO polymer composite against gamma-ray radiations. *Appl Radiat Isot.* 2025;**225**:111954. doi: 10.1016/j.apradiso.2025.111954. PubMed PMID: 40482542.
40. Safari A, Rafie P, Taeb S, Najafi M, Mortazavi SMJ. Development of Lead-Free Materials for Radiation Shielding in Medical Settings: A Review. *J Biomed Phys Eng.* 2024;**14**(3):229-44. doi: 10.31661/jbpe.v0i0.2404-1742. PubMed PMID: 39027711. PubMed PMCID: PMC11252547.
41. Mortazavi SMJ, Bevelacqua JJ, Rafiepour P, Sina S, Moradgholi J, Mortazavi SAR, Welsh JS. Lead-free, multilayered, and nanosized radiation shields in medical applications, industrial, and space research. In: Verma S, Srivastava AK, editors. Advanced Radiation Shielding Materials. Elsevier; 2024. p. 305-22.